1   **TITLE**
2   A generalizable epigenetic clock captures aging in two nonhuman primates.
3
4   **SHORT RUNNING TITLE**
5   A generalizable primate epigenetic clock
6
7   **AUTHORS**

8   Elisabeth A. Goldman[1]*[§] , Kenneth L. Chiou[2,3,4,5,] Marina M. Watowich[2,3,6], Arianne Mercer[4],
9   Sierra N. Sams[4], Julie E. Horvath[7,8,9,10], Jordan A. Anderson[10], Cayo Biobank Research Unit[^],
10   Jenny Tung[10,11,12,13,14], James P. Higham[15,16], Lauren J.N. Brent[17,] Melween I. Martínez[18], Michael
11   J. Montague[19], Michael L. Platt[19,20. 21], Kirstin N. Sterner[1]*+ & Noah Snyder-Mackler[2,3,4,5,22]*+
12

13   1.   Department of Anthropology, University of Oregon, Eugene, OR, USA.
14   2.   Center for Evolution and Medicine, Arizona State University, Tempe, AZ, USA.
15   3.   School of Life Sciences, Arizona State University, Tempe, AZ, USA.
16   4.   Department of Psychology, University of Washington, Seattle, WA, USA.
17   5.   Nathan Shock Center of Excellence in the Basic Biology of Aging, University of Washington, Seattle, WA,
18   USA.
19   6.   Department of Biology, University of Washington, Seattle, WA, USA.
20   7.   Department of Biological and Biomedical Sciences, North Carolina Central University, Durham, NC, USA.
21   8.   Genomics & Microbiology Research Lab, North Carolina Museum of Natural Sciences, Raleigh, NC, USA.
22   9.   Department of Biological Sciences, North Carolina State University, Raleigh, NC, USA.
23   10. Department of Evolutionary Anthropology, Duke University, Durham, NC, USA.
24   11. Department of Biology, Duke University, Durham, NC, USA.
25   12. Duke Population Research Institute, Duke University, Durham, NC, USA.
26   13. Canadian Institute for Advanced Research, Toronto, Ontario, Canada.
27   14. Department of Primate Behavior and Evolution, Max Planck Institute for Evolutionary Anthropology,
28   Leipzig, Germany.
29   15. Department of Anthropology, New York University, New York, NY, USA.
30   16. New York Consortium in Evolutionary Primatology, New York, NY, USA.
31   17. Centre for Research in Animal Behaviour, University of Exeter, Exeter, Devon, UK.
32   18. Caribbean Primate Research Center, University of Puerto Rico, San Juan, PR, USA.
33   19. Department of Neuroscience, University of Pennsylvania, Philadelphia, PA, USA.
34   20. Department of Psychology, University of Pennsylvania, Philadelphia, PA, USA.
35   21. Department of Marketing, University of Pennsylvania, Philadelphia, PA, USA.
36   22. Center for Studies in Demography & Ecology, University of Washington, Seattle, WA, USA.
37
38
39   ^Full list of consortium contributors included in supplement
40   +Equal contribution
41   *Correspondence to: goldmael@ohsu.edu, ksterner@uoregon.edu, nsnyderm@asu.edu
42
43

[§] E.A.G's current affiliation is Cancer Early Detection Advanced Research Center, Knight Cancer Institute, Oregon Health and Science University, Portland, OR.

ABSTRACT (250 words)

Epigenetic clocks generated from DNA methylation array data provide important insights into biological aging, disease susceptibility, and mortality risk. However, these clocks cannot be applied to high-throughput, sequence-based datasets more commonly used to study nonhuman animals. Here, we built a generalizable epigenetic clock using genome-wide DNA methylation data from 493 free-ranging rhesus macaques. Using a sliding-window approach that maximizes generalizability across datasets and species, this model predicted age with high accuracy ($\pm$ 1.42 years) in held-out test samples, as well as in two independent test sets: rhesus macaques from a captive population (n=43) and wild baboons in Kenya (n=271). Our model can also be used to generate insight into the factors hypothesized to alter epigenetic aging, including social status and exposure to traumatic events. Our results thus provide a flexible tool for predicting age in other populations and species and illustrate how connecting behavioral data with the epigenetic clock can uncover social influences on biological age.

KEY WORDS

DNA methylation; bisulfite sequencing; aging models; rhesus macaques; biological age

87
88   **INTRODUCTION**
89
90   Chronological age is the predominant risk factor for most chronic, non-communicable diseases.

91   However, chronological age *per se* cannot capture individual variation in health and disease risk

92   beyond that which is associated with the passage of time. Measures of biological age aim to

93   capture this variation to improve predictions of individual morbidity and mortality risk. The

94   epigenetic clocks constructed independently by Horvath (2013) and Hannum and colleagues

95   (2013) in humans were the first models of DNA methylation aging (also called epigenetic aging)

96   to gain widespread use. Work in humans has found that accelerated epigenetic aging–when

97   predicted biological age exceeds chronological age–is associated with increased risk of death (M.

98   E. Levine et al., 2018; Marioni et al., 2015, 2016) and increased susceptibility to several hallmark

99   diseases of aging (Ambatipudi et al., 2017; M. Levine et al., 2015; Wu et al., 2010; Yang et al.,

100   2016; Zheng et al., 2016). Epigenetic clocks are also responsive to socio-environmental

101   exposures associated with more rapid physiological and/or cognitive aging, such as trauma

102   incurred during active military combat (Boks et al., 2015), childhood adversity (Austin et al.,

103   2018; Marini et al., 2020; McCrory et al., 2022), and alcohol and tobacco use (Beach et al.,

104   2015). However, the pathways through which social and environmental factors "get under the

105   skin" to influence disparities in disease and mortality risk are difficult to investigate in humans

106   alone. The development of epigenetic clocks in nonhuman animal models can help address this

107   limitation by linking this promising tool to experimental studies, multigenerational field studies,

108   and comparative analyses across species.

109

110   Rhesus macaques (*Macaca mulatta*) and baboons (*Papio* spp.) are excellent models for human

111   aging because they are close evolutionary relatives for whom aging and survival are strongly

112   dependent on characteristics of the physical and social environment (Blomquist et al., 2011;

113   Chiou et al., 2020; Ellis et al., 2019). Such parallels are important because the impact of the

114   environment on the progression of aging may not manifest similarly in short-lived models of

115   mammalian aging, such as mice and rats. Indeed, questions that have been notoriously

116   challenging to study in humans can often be addressed in these closely related nonhuman

117   primates. For example, experimental life course studies in rhesus macaques have expanded our

118   understanding of the causal effects of dietary restriction on life- and healthspan (Colman et al.,

119   2014; Mattison et al., 2017). In addition, in social nonhuman primates, the association between

120   social status and indicators of aging and life expectancy mirror some aspects of the social

121   gradient of health in humans (Snyder-Mackler et al., 2020). Because nonhuman primate social

122   systems are variable (Abbott et al., 2003), studying different social conditions and positions in the

123   social hierarchy may point to specific variables that promote or detract from the impacts of

124   extrinsic challenges on an individual's health and survival.

125

126   The most extensively applied DNA methylation clocks to date (Hannum et al., 2013; Horvath,

127   2013) were built using DNA methylation data from humans generated on Illumina Infinium

128   microarrays. By contrast, many recent studies of DNA methylation in nonhuman organisms have

129   used high-throughput bisulfite sequencing (BS-seq) approaches (e.g., Chatterjee et al. 2013; Hahn

130   et al. 2017; Chen et al. 2015; Pegoraro et al. 2016; Platt et al. 2015; Stubbs et al. 2017; Wang et

131   al. 2017), for at least three reasons. First, while arrays designed for humans can sometimes be

132   applied in other nonhuman primates (Hernando-Herraez et al., 2013; Ong et al., 2014), doing so

133   requires stringent filtering for DNA sequence mismatches and changes in CpG site location,

134   reducing the amount of usable data relative to studies in humans (Pichon et al., 2021;

135   Teschendorff & Relton, 2018). Second, while designing species-specific arrays is also feasible,

136   such tailored tools are often higher in cost. Third, many researchers have been interested not only

137   in epigenetic aging, but also in patterns of differential methylation (e.g., age, genotype, or

138   environment-related), which sometimes occur outside of the regions traditionally targeted by

139   DNA methylation arrays (W. Zhang et al., 2015; Y. Zhang et al., 2016). Notably, this limitation

140   also applies to recently developed multi-species arrays like the HorvathMammalMethylChip

141   (Arneson et al., 2021). The multi-species array has provided extensive insight into epigenetic

142   aging across many mammals (e.g., Horvath et al. 2022; Wilkinson et al. 2021) while capturing

143   DNA methylation at only 38,000 highly conserved, non-randomly distributed CpG sites.

144   Consequently, generalizable tools to study epigenetic aging using BS-seq data are also needed.

145   Here, we developed the RheMacAge model, a nonhuman primate epigenetic clock that facilitates

146   comparisons among Old World monkey species often used as models for human aging. We first

147   developed a generalizable epigenetic clock model that can predict chronological age using BS-

148   seq data with high accuracy. Next, we applied our model to two independently generated datasets

149   to demonstrate not only the cross-*study* but cross-*species* applicability of our approach in two

150   nonhuman primates with exceptional research importance, rhesus macaques and baboons. Finally,

151   we used the model to test whether social status or exposure to an adverse climate event were

152   associated with variation in epigenetic aging.

153

MATERIALS AND METHODS

Study Population and Sample Collection

Our primary dataset consisted of 563 whole blood samples (number of unique individuals=493) collected from rhesus macaques living on Cayo Santiago, an island 1 km off the coast of Puerto Rico that is home to over 1,800 free-ranging rhesus macaques. The population is managed by the Caribbean Primate Research Center (CPRC) as part of a long-term field station in operation since 1938. The macaques are provisioned with food and water but are otherwise allowed to roam freely, self-organize into social groups, and do not face the threat of predation (Rawlins & Kessler, 1986). Collectively, these conditions provide opportunities to investigate how interactions between ecology and behavior influence environmentally-responsive molecular mechanisms (such as DNA methylation) in the absence of other confounding factors (e.g., variable nutrition and predation).

The data in this study were collected from 273 female and 220 male rhesus macaques, aged 1.44 months to 28.82 years (birth dates recorded by CPRC census takers). We collected blood samples and behavioral data on these animals between 2010 to 2018 (with the exception of 2017, when sampling was not possible due to Hurricane Maria). On Cayo Santiago, the average age at sexual maturity for a female is 4 years, and median lifespan for an adult female is 18 years (Chiou et al., 2020). By comparison, human females in the United States reach sexual maturity at an average

6

175   age of 14 years (Susman et al., 2010) and have a median lifespan of 80.5 years (National Center

176   for Health Statistics 2021) .

177

178   Sixty-six individuals were sampled more than once during this study (see **Supplemental File 2**

179   for detailed metadata). Blood was collected into K3 EDTA vacutainer tubes (BD Biosciences,

180   Franklin Lakes, NJ) and placed on ice until storage at -80°C (within 8 hours of collection). All

181   work was reviewed and approved by the Institutional Animal Care and Use Committees of the

182   University of Washington (assurance number A3464-01) and the University of Puerto Rico,

183   Medical Sciences Campus (assurance number A4001-17). This work also adheres to the

184   American Society of Primatologists Principles for the Ethical Treatment of Nonhuman Primates.

185

186   *RRBS Data Generation*

187

188   Genomic DNA was isolated from whole blood using the Qiagen Blood and Tissue DNA kit

189   (QIAGEN, Hilden, Germany). To measure CpG methylation, we used Reduced Representation

190   Bisulfite Sequencing (RRBS), a version of bisulfite sequencing (BS-seq) that uses an initial

191   restriction enzyme digest to concentrate sequencing in and near CpG-rich regions of the genome

192   (Gu et al., 2011; Meissner, 2005).To prepare RRBS libraries, we followed the library preparation

193   protocol detailed on the Snyder-Mackler Lab website (https://smack-lab.com/wp-

194   content/uploads/2020/03/SMack_Lab_RRBS-with-Zymo-EZDNA-MagBead.pdf). Briefly, we

195   digested extracted DNA using the *Msp1* restriction enzyme, which cuts at CCGG sites, ligated

196   NEBNext methylated adapters (Illumina Inc., San Diego, CA), bisulfite converted the DNA using

7

197   the Zymo EZDNA Methylation- Lightning™ Kit (Zymo Research, Irvine, CA), and PCR-

198   amplified the final fragments with unique dual molecular indices for each sample. RRBS libraries

199   were sequenced in two batches. Batch 1 contained 104 samples (2x50bp reads) sequenced on an

200   Illumina NovaSeq S2 flowcell. Batch 2 was made up of 527 samples (2x100bp reads) and

201   sequenced on a NovaSeq S4 flowcell.

202

203   *Alignment and Preprocessing*

204

205   We trimmed adapter and low-quality sequences with TrimGalore! (v0.4.5) (Martin, 2011). We

206   then aligned trimmed reads to the *in silico* bisulfite-converted reference genome (Mmul10) using

207   the default settings in Bismark (v0.20.0) (Krueger & Andrews, 2011) for all but two parameters (-

208   -score-min and -R; see the **Methods Supplement**). We parallelized sample aggregation with

209   GNU parallel (Tange, 2018) and BedTools (v2.24.0) (Quinlan & Hall, 2010). Unless otherwise

210   stated, all subsequent analyses were carried out in RStudio (v1.4.1106) (RStudio Team, 2015).

211

212   *Development of a Generalizable Epigenetic Clock*

213

214   Site-based modeling approach

215   To limit the inclusion of invariant or uninformative sites, we first removed CpG sites with

216   missing data in more than 10% of the training samples and samples missing more than 25% of

217   CpG sites in the filtered dataset. Next, we removed constitutively hypo- or hypermethylated sites

218   (those with median percent methylation less than 10% or greater than 90% across samples), and

8

219   sites with less than 5X median coverage, resulting in 196,345 CpG sites in the site-based dataset.

220   A detailed description of sample filtering criteria can be found in the **Methods Supplement**.

221

222   Next, we imputed missing and low coverage (< 5X) sites in the 196,345 CpG site dataset using

223   BoostMe (v0.1.0) (L. S. Zou et al., 2018). On average, 12.5% of sites were imputed per sample.

224   After removing sites mapping to sex chromosomes and those containing one or more

225   inadmissible values (non-real numbers that result from when BoostMe attempts to divide by

226   zero), the dataset contained 185,153 unique CpG sites.

227

228   Sliding window-based modeling approach

229   To improve model generalizability, we compared the performance of a traditional site-based

230   model to a 1 Kb, non-overlapping sliding-window based approach that we reasoned might

231   capture more shared loci across samples and datasets. In each 1 Kb window of the genome, we

232   calculated the percent methylation for a given sample as the number of reads covering methylated

233   CpG sites, divided by the total number of reads covering CpG sites in that window. We

234   implemented the same filtering strategy described above by excluding windows that had missing

235   data in more than 10% of samples (leaving 279,052 windows), samples that were missing data for

236   more than 25% of windows in the dataset, windows that were constitutively hypo- or

237   hypermethylated, and those with less than 5X median coverage, leaving a final set of 161,289

238   windows.

239

240   Missing values and those with < 5X coverage at a given site were imputed using BoostMe. The

241   average proportion of imputed windows was 1.98% per sample and ranged from 0.05% to 23.2%.

242   Notably, the average proportion of features imputed for the window-based approach was six-fold

243   lower than that for the site-based dataset (1.98% as compared to 12.5%). Following imputation,

244   removal of windows containing non-real numbers, and removal of those mapping to sex

245   chromosomes, 159,472 windows were retained for calibrating the epigenetic clock.

246   All three datasets used to train, validate, and/or test the model were processed in an identical

247   manner.

248

249   *Model Training and Optimization*

250

251   We then generated age-prediction models independently for the site-based and window-based

252   datasets. We used elastic net regression implemented using the R package glmnet (v4.1-1)

253   (Friedman et al., 2010) and leave-one-out cross validation (LOOCV) to train our model. To

254   perform LOOCV, one sample was held out at a time, and 'proto-models' were generated on the

255   remaining N-1 samples using 10-fold internal cross validation. The "best" proto-model (the

256   proto-model with the lowest mean absolute error) was then used to predict the age of the held-out

257   sample. This process was repeated for each sample in the dataset. Once all 563 age predictions

258   were generated, we regressed all predicted age values onto known chronological ages to evaluate

259   the predictive performance of the dataset in our primary dataset.

260

261   We defined a measure of age acceleration, termed "residual epigenetic age" (similar to Horvath's

262   [2013] "delta age") by taking the residuals from a loess (locally estimated scatterplot smoothing;

263   span = 0.75) regression of predicted onto chronological age to identify individuals who appear to

264   be aging more (or less) rapidly than expected given their chronological age. By taking the

265   residuals from a loess regression, we can detect potentially meaningful deviations from the

266   expected rate of aging while accounting for systemic effects of the model (e.g., the influence of

267   chronological age) and non-linear pace of epigenetic aging. We adjusted for a marginally

268   significant effect of sex on epigenetic age ($p = 0.05$) by calculating residual epigenetic age for

269   females and males separately.

270

271   *Model Validation in Independent Datasets*

272

273   We sought to test the generalizability and performance of both the site- and window-based

274   models ("Cayo" models) using two independently generated RRBS datasets ("Yerkes" and

275   "baboon" datasets). However, the site-based model's applicability was constrained by the limited

276   overlap between the site-based RRBS independent datasets (**Figure S1**).

277

278   To test the generalizability of the window-based model to populations and study systems of the

279   same species, we used samples from 43 female rhesus macaques, aged 3.1 to 20.1 years, housed

280   at Yerkes National Primate Research Center. RRBS libraries were generated from purified

281   classical monocytes (CD3$^-$/CD14$^+$) collected in an unrelated study examining dominance rank

282   effects on gene regulation and immune function (Snyder-Mackler et al., 2016). Second, to test

283   generalizability in another important model for human aging, we applied our model to a second

284   RRBS dataset generated from 271 whole blood samples collected from wild baboons living in

285   Amboseli National Park in Kenya (Anderson et al., 2021) (SRA project accession

286   PRJNA648767). This dataset contains samples collected from 138 females and 133 males, aged

287   1.93 to 26.34 years. The data processing workflow was identical across the Cayo, Yerkes, and

288   baboon datasets.

289

290   To generate a single epigenetic clock for predicting age in independent datasets, we quantile

291   normalized methylation values across features and across samples independently for the Yerkes

292   macaque and Amboseli baboon datasets. Next, we determined optimal hyperparameter settings

293   using the caret package (v6.0-86) (Kuhn, 2019, https://topepo.github.io/caret/) by performing a

294   grid search across two hundred combinations of alpha (the parameter that controls how similar

295   the model is to lasso versus ridge regression ((H. Zou & Hastie, 2005) and lambda (the

296   regularization parameter) using repeated (3x) 10-fold cross validation on all 563 Cayo samples.

297   After LOOCV models were generated, we performed an elastic net regression with the optimized

298   hyperparameter values on the entire dataset and applied the resulting model to the two external

299   datasets (Yerkes and baboon).

300

301   *Effects of Social and Environmental Adversity on Epigenetic Aging*

302

303   To explore how heterogeneity in the social environment is reflected in biological aging, we tested

304   the relationship between dominance rank and epigenetic aging in the Cayo Santiago rhesus

305   macaque samples. First, we quantified dominance rank for 81 males and 116 females from dyadic

306   win-loss interactions between individuals within a social group using behavioral data collected

307   prior to each blood draw. The dominance rank of an individual represents the proportion of same-

308   sex individuals in their group that they out-ranked. In 2010-2014, the trap and release season was

309   Jan-Mar, and rank data were calculated from behavioral data recorded in April-Dec of the

310   previous year. In late 2014 until 2018, the trap and release season was moved to Oct–Dec. For

311   samples collected in this time period, rank data were thus calculated from behavioral data

312   recorded in Jan–Oct of the same calendar year. Next, we tested if dominance rank is associated

313   with epigenetic age by modeling residual epigenetic age as a function of dominance rank for

314   females (aged 6.01 – 27.93 years) and males (aged 5.89 – 22.78 years) separately. Additionally,

315   we tested whether residual epigenetic age was driven by length of tenure in the social group

316   among males in a larger subset of the Cayo Santiago population (n = 230, aged 3.86– 21.74

317   years). Rhesus macaque males attain their dominance largely via queueing instead of direct

318   contest such that longer residency times predict higher rank (Kimock et al., 2019, 2022). Tenure

319   length is thus a useful proxy of male rank and is advantageous as a measure because demographic

320   records have been collected over a longer period of time compared to behavioral data.

321

322   Finally, motivated by the observation that Cayo Santiago macaques that survived Hurricane

323   Maria in 2017 exhibited "aged" blood transcriptomes (Watowich et al., 2022), we tested if

324   Hurricane Maria had left a similar mark in epigenetic age. To do so, we modeled residual

325   epigenetic age as a function of exposure to Hurricane Maria for all adult animals (aged at least 4

13

326   years). We excluded infants and juveniles due to previously observed differences in the rate of

327   aging between human adults versus children and adolescents (Horvath, 2013).

328

329   **RESULTS**

330

331   RheMacAge *is a generalizable epigenetic clock that accurately predicts chronological age.*

332

333   Although our site-based model was able to accurately predict age (Pearson's r = 0.82 MAD =

334   2.11 years) **(Figure 1A),** it was significantly outperformed by the window-based model

335   (Pearson's r = 0.9, MAD = 1.42 years; 0.69-year difference in MAD between two models, $p_{t\text{-}test}$ =

336   5.36 x 10^{-8}) (**Figure 1B**). The window-based model performed equally well in males and females

337   ($p_{t\text{-}test}$ = 0.71). While both models predicted chronological age well, their predictions did not scale

338   linearly with chronological age. Age predictions plateau at older ages (> 20 years among the

339   macaques in our Cayo sample), as has been reported in other species, including humans (e.g.,

340   Levine et al. 2020; Horvath 2013).

341

342   Although the site- and window-based datasets contained a similar number of loci after filtering

343   within the Cayo data (~180K and ~160K, respectively), when applying these models to the

344   external Yerkes data set, the overlap in features retained in both datasets was much higher when

345   we used the window-based approach. Of the 185,153 CpG sites in the filtered Cayo dataset, 38%

346   (70,439) of sites also passed the same filters in the Yerkes dataset, compared to 97% (155,347) of

347   shared features for the window-based dataset (**Figure S1).** Given that the window-based model

14

348   also showed superior performance in predicting age in the Cayo population, we used the window-

349   based RheMacAge clock for all subsequent analyses.

350

351   The RheMacAge clock included 359 windows, of which 164 decreased in methylation with age

352   ("hypomethylated windows") and 195 increased in methylation with age ("hypermethylated

353   windows"). CpG sites that exhibit age-dependent changes in methylation are often found in

354   evolutionarily conserved regions of the genome (Mozhui & Pandey, 2017), and certain age-

355   dependent patterns of methylation change are conserved between humans and mice (Spiers et al.,

356   2016; Stubbs et al., 2017). Indeed, windows in the RheMacAge clock were modestly but

357   significantly more evolutionarily conserved than windows that were not part of the clock (D =

358   0.09, p = 0.007, two-sample Kolmogorov-Smirnov test) (**Figures S2, S3**).

359

360   Since we collected repeated samples from 66 individuals, we were able to test if our model

361   accurately tracked aging within an individual. For these 66 individuals (n=70 paired samples,

362   because 4 individuals were sampled three times), 88.6% (62/70) exhibited increased biological

363   age with increased chronological age (**Figure 2**). Thus, samples collected later in time were

364   consistently predicted to be older than those collected at earlier points in time (p = 9.13 x 10^{-12},

365   one-sided exact binomial test).

366

367   *The RheMacAge clock predicts age in two independent datasets, demonstrating cross-study and*

368   *cross-species applicability.*

369

15

370   We evaluated our model ("Cayo") in an independent macaque sample comprised of 43 female

371   rhesus macaques from the "Yerkes" dataset (aged 3.1 to 20.1 years). DNA methylation-based age

372   predictions were significantly correlated with chronological age (**Figure 3**) (Pearson's r = 0.69, p

373    $= 2.65 \times 10^{-7}$), with an MAD of 2.09 years. This suggests the RheMacAge clock can be

374   generalized to predict age in rhesus macaque data generated from different populations and

375   different cell types (monocytes versus all white blood cells), and by different laboratories.

376

377   When applied to individuals from our "baboon" dataset (aged 1.93 to 26.34 years), the

378   RheMacAge clock was also able to predict chronological age surprisingly well, producing the

379   same sex-specific patterns in the rate of aging described in previous work (Anderson et al., 2021).

380   Specifically, prediction was better for male baboons than female baboons, especially at older ages

381   (male Pearson's r = 0.8, $p < 2.2 \times 10^{-16}$; MAD = 1.34 years, **Figure 4A**; female Pearson's r =

382   0.74, $p < 2.2 \times 10^{-16}$; MAD = 2.19 years, **Figure 4B**). The RheMacAge clock predictions for

383   baboons were not as accurate as a baboon-specific model (baboon clock: male MAD = 0.85

384   years, female MAD = 1.6 years). Importantly, the RheMacAge clock captured a similar

385   biological signal to the baboon clock: residual epigenetic ages calculated from both models were

386   significantly positively correlated for both sexes (males: r = 0.55, $p = 5.28 \times 10^{-12}$; females: r =

387   0.41, $p = 7.49 \times 10^{-7}$; **Figures 4C** and **4D**). In addition, for male baboons, estimates of residual

388   epigenetic age generated using the RheMacAge clock replicated the significant association (first

389   reported in Anderson et al., 2021) between high social status and older epigenetic age (Pearson's

390   r = -0.47, $p = 4.05 \times 10^{-7}$, n = 104; the correlation is negative because lower values on an ordinal

16

391   rank measure represent higher status). We found no significant association between rank and

392   epigenetic age in female baboons.

393

394   *Epigenetic age predictions for the Cayo macaques showed no association with social and*

395   *environmental variables tested.*

396

397   We identified no association between residual epigenetic age and dominance rank in adult male

398   (n = 60, β = -0.22, *p* = 0.3) or female (n = 83, β = -0.05, *p* = 0.77) rhesus macaques from Cayo

399   Santiago. Residual epigenetic age in males also did not correlate with group tenure length (n =

400   59, β = -0.23, *p* = 0.33). Finally, contrary to our prediction, we found no relationship between

401   hurricane exposure and residual epigenetic age (*p* = 0.24).

402

403   **DISCUSSION**

404

405   *The RheMacAge clock accurately captures chronological and biological aging in two nonhuman*

406   *primate models for human aging and offers a generalizable approach that can be used when*

407   *developing epigenetic clock models from BS-seq data.*

408

409   Rhesus macaques and baboons are important biomedical models for human aging (Chiou et al.,

410   2020; Huber et al., 2020). However, there are comparatively fewer 'omics' resources available

411   for either species than for humans or mice (see Meer et al., 2018). To partially address this gap,

412   here we present genome-wide DNA methylation data from 563 rhesus macaque samples along

17

413   with new analyses of previously published data from 43 rhesus macaques and 271 baboons. The

414   present study thus represents the largest study of DNA methylation carried out to date in

415   nonhuman primates.

416

417   Our RheMacAge clock produced accurate age estimates from blood in an independent sample of

418   captive female rhesus macaques and a large sample of wild baboons. We also observed a more

419   rapid rate of epigenetic change with age in males versus female baboons that is consistent with

420   results from Anderson et al. (2021), demonstrating that our approach can capture similar aging

421   signatures across species. As such, the model serves as a useful biomarker of aging in blood that

422   can facilitate research on the causes and consequences of the aging process. While the

423   RheMacAge clock was only tested in two species, it may be suitable for application other

424   primates (e.g., long-tailed macaques, sooty mangabeys) that are closely related to rhesus

425   macaques and baboons. In addition, we offer a more generalizable approach that can be used

426   when developing epigenetic clock models from BS-seq data more commonly generated from

427   nonhuman animals.

428

429   *Species-specific socioecology is reflected in variation in epigenetic aging in baboons and*

430   *macaques.*

431

432   We found no significant relationship between epigenetic aging and dominance rank in female or

433   male rhesus macaques. This result differs from the effect described in male baboons, where high-

434   ranking males exhibited older relative epigenetic ages compared to lower-ranking males

18

435   (Anderson et al., 2021). On the surface, these findings appear discordant, but they may be a

436   legitimate reflection of differences in dominance rank acquisition between rhesus macaques and

437   baboons. Specifically, in the Amboseli baboons, male rank is determined by competitive

438   interactions and mating occurs throughout the year. Maintaining alpha status requires significant

439   energy expenditure during mate guarding and competition with other males, and alpha males

440   have the highest glucocorticoid levels across the male status hierarchy (Alberts et al., 2006;

441   Gesquiere et al., 2011). In contrast, male rhesus macaques obtain high social status through a less

442   physically competitive queueing system in which males rise in rank as their tenure in a social

443   group lengthens (Berard, 1999). Rhesus macaques are also seasonal breeders, meaning that direct

444   male investment in mating effort is restricted to several months of the year (Bercovitch, 1997).

445   Consequently, high status is not as difficult or energetically expensive to maintain in male rhesus

446   macaques as it is in male baboons, and status in rhesus males is more predictable. Together, these

447   species differences in the male competitive regime predict that high rank in male baboons is more

448   energetically taxing, while high rank in rhesus males may be less stressful and/or demanding

449   compared to lower ranking positions (Sapolsky, 2005). These differences point to strategies of

450   mitigating distinct types of social stress as one mechanism that may be involved in dictating the

451   rate at which the biological clock 'ticks'.

452

453   Surprisingly, although exposure to Hurricane Maria was associated with accelerated

454   immunological aging in the Cayo rhesus macaque transcriptome (Watowich et al., 2022), it was

455   not significantly associated with residual epigenetic age in our study. One possible explanation

456   for these observations is that the mechanisms underlying the clock are distinct from those that

19

457   regulate age-related changes in the immune response (see Bell et al., 2019 for discussion of

458   mechanisms). Further, the extent and velocity at which DNA methylation changes at sites

459   typically captured in epigenetic clocks following exposure to adverse events is not known. Future

460   studies will help enhance our knowledge of what factors are and are not involved in regulating

461   the progression of epigenetic aging.

462

463   *Future Directions*

464

465   The RheMacAge model has the potential to complement and expand aging research in primate

466   populations. Our model can be used to test the effects of medical interventions intended to delay

467   age-related physiological decline, such as caloric restriction, rapamycin administration, or other

468   pharmacological treatments, where studies in macaques or baboons are ongoing (e.g.,

469   Tarandovskiy et al., 2020). It is also particularly well-suited to situations where environment and

470   behavior intersect. For example, the model could be used to examine whether adversity

471   experienced early in life is linked to late-life changes in the pace of biological aging. Such

472   research could uncover molecular mechanisms that regulate how stressors become biologically

473   embedded and may help identify health or behavioral variables that contribute to increased

474   resiliency. Finally, our findings highlight the utility of the RheMacAge clock for disentangling

475   when and to what extent social factors influence the pace of aging. The ability to apply the same

476   predictive model across species facilitates comparative work, which in turn highlights how

477   variation in social hierarchies translates into variation in their physiological correlates.

478

20

479   Excitingly, the RheMacAge clock comes online at a time when resources for studying epigenetic

480   aging in nonhuman mammals are expanding more generally. For example, the

481   HorvathMammalMethylChip has already been deployed to study the effects of hibernation on

482   epigenetic aging in yellow-bellied marmots (Pinho et al., 2022), to examine postnatal

483   development of the epigenome in opossums and other marsupials (Horvath et al., 2022), and to

484   evaluate the potential lifespan-extending effects of partial cell reprogramming in a mouse model

485   of premature aging (Browder et al., 2022). Our RheMacAge model, which takes a sliding-

486   window approach, provides a useful alternative to the HorvathMammalMethylChip for

487   researchers who wish to look at how DNA methylation varies across the genome more broadly,

488   by coupling applications of the clock with differential or allele-specific methylation analyses. In

489   mammals, RRBS datasets typically profile upwards of ~500,000 CpG sites after quality control,

490   as opposed to the 38,000 CpG sites on the chip. Additionally, RRBS datasets are more likely to

491   contain sites that are specific to the species of interest, as CpG sites that are not as tightly

492   conserved are often the most interesting from an evolutionary perspective. Future work that

493   calibrates the epigenetic clock using blood chemistry or other relevant biological measures of

494   aging to predict physiological decline and/or mortality, as the human "next-generation" clocks

495   have found success in doing (e.g., Belsky et al. 2020; Levine et al. 2018; Lu et al. 2019), has the

496   potential to further extend the applicability of these models. Together, these methods contribute

497   to an important and growing analytical toolkit for research in nonhuman primates.

498

499   **CONCLUSIONS**

500

501 We have developed a method that overcomes a persistent barrier to comparative analyses using

502 BS-seq datasets. Our approach is easy to implement and the generalizability of the resulting

503 model enables cross-study comparison, as demonstrated by the successful application of our

504 RheMacAge model to independent RRBS datasets to predict age in two distinct species. Our

505 model recapitulated a previously identified relationship between rank and epigenetic aging in

506 wild male baboons (Anderson et al., 2021) but found no such effect in male rhesus macaques,

507 suggesting the importance of the way dominance hierarchies are formed and maintained in

508 different species. These results provide proof-of-concept for our model and its capacity to

509 measure the influence of the social and ecological environment on health, aging, disease and

510 mortality risk. Despite numerous attempts to decipher the underlying mechanisms of the clock,

511 they remain largely obscure. However, such knowledge is not required to use the clock to

512 continue to probe environmental variables that accelerate or decelerate the pace of aging. The

513 increasingly widespread use of epigenetic clock models has advanced the field towards an

514 essential goal: quantification of the impact of lived experiences on health and aging. Future

515 research should aim to identify specific variables that have the greatest impact on health and

516 longevity. We anticipate that our model will facilitate interrogation of novel socio-environmental

517 factors and whether they are or are *not* able to effectively "get under the skin" to engender

518 epigenetic change, and how these modifications fit into the larger, systemic picture of aging and

519 longevity across species.

520

521 **ACKNOWLEDGEMENTS**

522

22

537
538

REFERENCES

Abbott, D. H., Keverne, E. B., Bercovitch, F. B., Shively, C. A., Mendoza, S. P., Saltzman, W., Snowdon, C. T., Ziegler, T. E., Banjevic, M., Garland, T., & Sapolsky, R. M. (2003). Are subordinates always stressed? A comparative analysis of rank differences in cortisol levels among primates. *Hormones and Behavior*, *43*(1), 67–82. https://doi.org/10.1016/S0018-506X(02)00037-5

Alberts, S. C., Buchan, J. C., & Altmann, J. (2006). Sexual selection in wild baboons: From mating opportunities to paternity success. *Animal Behaviour*, *72*(5), 1177–1196. https://doi.org/10.1016/j.anbehav.2006.05.001

Ambatipudi, S., Horvath, S., Perrier, F., Cuenin, C., Hernandez-Vargas, H., Le Calvez-Kelm, F., Durand, G., Byrnes, G., Ferrari, P., Bouaoun, L., Sklias, A., Chajes, V., Overvad, K., Severi, G., Baglietto, L., Clavel-Chapelon, F., Kaaks, R., Barrdahl, M., Boeing, H., … Herceg, Z. (2017). DNA methylome analysis identifies accelerated epigenetic ageing associated with postmenopausal breast cancer susceptibility. *European Journal of Cancer*, *75*, 299–307. https://doi.org/10.1016/j.ejca.2017.01.014

Anderson, J. A., Johnston, R. A., Lea, A. J., Campos, F. A., Voyles, T. N., Akinyi, M. Y., Alberts, S. C., Archie, E. A., & Tung, J. (2021). High social status males experience accelerated epigenetic aging in wild baboons. *ELife*, *10*, e66128. https://doi.org/10.7554/eLife.66128

Arneson, A., Haghani, A., Thompson, M. J., Pellegrini, M., Kwon, S. B., Vu, H., Yao, M., Li, C. Z., Lu, A. T., Barnes, B., Hansen, K. D., Zhou, W., Breeze, C. E., Ernst, J., & Horvath, S. (2021). *A mammalian methylation array for profiling methylation levels at conserved sequences* [Preprint]. Bioinformatics. https://doi.org/10.1101/2021.01.07.425637

Austin, M. K., Chen, E., Ross, K. M., McEwen, L. M., MacIsaac, J. L., Kobor, M. S., & Miller, G. E. (2018). Early-life socioeconomic disadvantage, not current, predicts accelerated epigenetic aging of monocytes. *Psychoneuroendocrinology*, *97*, 131–134. https://doi.org/10.1016/j.psyneuen.2018.07.007

Beach, S. R. H., Dogan, M. V., Lei, M.-K., Cutrona, C. E., Gerrard, M., Gibbons, F. X., Simons, R. L., Brody, G. H., & Philibert, R. A. (2015). Methylomic Aging as a Window onto the Influence of Lifestyle: Tobacco and Alcohol Use Alter the Rate of Biological Aging. *Journal of the American Geriatrics Society*, *63*(12), 2519–2525. https://doi.org/10.1111/jgs.13830

Belsky, D. W., Caspi, A., Arseneault, L., Baccarelli, A., Corcoran, D. L., Gao, X., Hannon, E., Harrington, H. L., Rasmussen, L. J., Houts, R., Huffman, K., Kraus, W. E., Kwon, D., Mill, J., Pieper, C. F., Prinz, J. A., Poulton, R., Schwartz, J., Sugden, K., … Moffitt, T. E. (2020). Quantification of the pace of biological aging in humans through a blood test, the DunedinPoAm DNA methylation algorithm. *ELife*, *9*, e54870. https://doi.org/10.7554/eLife.54870

Berard, J. (1999). A four-year study of the association between male dominance rank, residency status, and reproductive activity in rhesus macaques (Macaca mulatta). *Primates*, *40*(1), 159–175. https://doi.org/10.1007/BF02557708

Bercovitch, F. B. (1997). Reproductive strategies of rhesus macaques. *Primates*, *38*(3), 247–263. https://doi.org/10/chqcwg

Blomquist, G. E., Sade, D. S., & Berard, J. D. (2011). Rank-Related Fitness Differences and Their Demographic Pathways in Semi-Free-Ranging Rhesus Macaques (Macaca mulatta). *International Journal of Primatology*, *32*(1), 193–208. https://doi.org/10/bd6hxh

Boks, M. P., Mierlo, H. C. van, Rutten, B. P. F., Radstake, T. R. D. J., De Witte, L., Geuze, E., Horvath, S., Schalkwyk, L. C., Vinkers, C. H., Broen, J. C. A., & Vermetten, E. (2015). Longitudinal changes of telomere length and epigenetic age related to traumatic stress and post-traumatic stress disorder. *Psychoneuroendocrinology*, *51*, 506–512. https://doi.org/10.1016/j.psyneuen.2014.07.011

Browder, K. C., Reddy, P., Yamamoto, M., Haghani, A., Guillen, I. G., Sahu, S., Wang, C., Luque, Y., Prieto, J., Shi, L., Shojima, K., Hishida, T., Lai, Z., Li, Q., Choudhury, F. K., Wong, W. R., Liang, Y., Sangaraju, D., Sandoval, W., … Izpisua Belmonte, J. C. (2022). In vivo partial reprogramming alters age-associated molecular changes during physiological aging in mice. *Nature Aging*, *2*(3), 243–253. https://doi.org/10.1038/s43587-022-00183-2

Chatterjee, A., Ozaki, Y., Stockwell, P. A., Horsfield, J. A., Morison, I. M., & Nakagawa, S. (2013). Mapping the zebrafish brain methylome using reduced representation bisulfite sequencing. *Epigenetics*, *8*(9), 979–989. https://doi.org/10.4161/epi.25797

Chen, X., Ge, X., Wang, J., Tan, C., King, G. J., & Liu, K. (2015). Genome-wide DNA methylation profiling by modified reduced representation bisulfite sequencing in Brassica rapa suggests that epigenetic modifications play a key role in polyploid genome evolution. *Frontiers in Plant Science*, *6*. https://doi.org/10.3389/fpls.2015.00836

Chiou, K. L., Montague, M. J., Goldman, E. A., Watowich, M. M., Sams, S. N., Song, J., Horvath, J. E., Sterner, K. N., Ruiz-Lambides, A. V., Martínez, M. I., Higham, J. P., Brent, L. J. N., Platt, M. L., & Snyder-Mackler, N. (2020). Rhesus macaques as a tractable physiological model of human ageing. *Philosophical Transactions of the Royal Society B: Biological Sciences*, *375*(1811), 20190612. https://doi.org/10.1098/rstb.2019.0612

Colman, R. J., Beasley, T. M., Kemnitz, J. W., Johnson, S. C., Weindruch, R., & Anderson, R. M. (2014). Caloric restriction reduces age-related and all-cause mortality in rhesus monkeys. *Nature Communications*, *5*(1), 3557. https://doi.org/10.1038/ncomms4557

Ellis, S., Snyder-Mackler, N., Ruiz-Lambides, A., Platt, M. L., & Brent, L. J. N. (2019). Deconstructing sociality: The types of social connections that predict longevity in a group-living primate. *Proceedings of the Royal Society B: Biological Sciences*, *286*(1917), 20191991. https://doi.org/10.1098/rspb.2019.1991

616   Friedman, J., Hastie, T., & Tibshirani, R. (2010). Regularization Paths for Generalized Linear
617   Models via Coordinate Descent. *Journal of Statistical Software*, *33*(1).
618   https://doi.org/10.18637/jss.v033.i01

619   Gesquiere, L. R., Learn, N. H., Simao, M. C. M., Onyango, P. O., Alberts, S. C., & Altmann, J.
620   (2011). Life at the Top: Rank and Stress in Wild Male Baboons. *Science*, *333*(6040), 357–
621   360. https://doi.org/10/ft7zkf

622   Gu, H., Smith, Z. D., Bock, C., Boyle, P., Gnirke, A., & Meissner, A. (2011). Preparation of
623   reduced representation bisulfite sequencing libraries for genome-scale DNA methylation
624   profiling. *Nature Protocols*, *6*(4), 468–481. https://doi.org/10.1038/nprot.2010.190

625   Hahn, O., Grönke, S., Stubbs, T. M., Ficz, G., Hendrich, O., Krueger, F., Andrews, S., Zhang, Q.,
626   Wakelam, M. J., Beyer, A., Reik, W., & Partridge, L. (2017). Dietary restriction protects
627   from age-associated DNA methylation and induces epigenetic reprogramming of lipid
628   metabolism. *Genome Biology*, *18*(1). https://doi.org/10.1186/s13059-017-1187-1

629   Hannum, G., Guinney, J., Zhao, L., Zhang, L., Hughes, G., Sadda, S., Klotzle, B., Bibikova, M.,
630   Fan, J.-B., Gao, Y., Deconde, R., Chen, M., Rajapakse, I., Friend, S., Ideker, T., & Zhang,
631   K. (2013). Genome-wide Methylation Profiles Reveal Quantitative Views of Human
632   Aging Rates. *Molecular Cell*, *49*(2), 359–367.
633   https://doi.org/10.1016/j.molcel.2012.10.016

634   Hernando-Herraez, I., Prado-Martinez, J., Garg, P., Fernandez-Callejo, M., Heyn, H., Hvilsom,
635   C., Navarro, A., Esteller, M., Sharp, A. J., & Marques-Bonet, T. (2013). Dynamics of
636   DNA Methylation in Recent Human and Great Ape Evolution. *PLoS Genetics*, *9*(9),
637   e1003763. https://doi.org/10.1371/journal.pgen.1003763

638   Horvath, S. (2013). DNA methylation age of human tissues and cell types. *Genome Biology*,
639   *14*(10), R115. https://doi.org/10.1186/gb-2013-14-10-r115

640   Horvath, S., Haghani, A., Zoller, J. A., Raj, K., Sinha, I., Robeck, T. R., Black, P., Couzens, A.,
641   Lau, C., Manoyan, M., Ruiz, Y. A., Talbott, A., Belov, K., Hogg, C. J., & Sears, K. E.
642   (2022). Epigenetic clock and methylation studies in marsupials: Opossums, Tasmanian
643   devils, kangaroos, and wallabies. *GeroScience*, *44*(3), 1825–1845.
644   https://doi.org/10.1007/s11357-022-00569-5

645   Huber, H. F., Jenkins, S. L., Li, C., & Nathanielsz, P. W. (2020). Strength of nonhuman primate
646   studies of developmental programming: Review of sample sizes, challenges, and steps for
647   future work. *Journal of Developmental Origins of Health and Disease*, *11*(3), 297–306.
648   https://doi.org/10.1017/S2040174419000539

649   Kimock, C. M., Brent, L. J. N., Dubuc, C., & Higham, J. P. (2022). Body size and canine size do
650   not confer a competitive advantage in male rhesus macaques. *Animal Behaviour*, *187*,
651   281–290. https://doi.org/10.1016/j.anbehav.2022.01.011

652   Kimock, C. M., Dubuc, C., Brent, L. J. N., & Higham, J. P. (2019). Male morphological traits are
653   heritable but do not predict reproductive success in a sexually-dimorphic primate.
654   *Scientific Reports*, *9*(1), 19794. https://doi.org/10.1038/s41598-019-52633-4

655 Krueger, F., & Andrews, S. R. (2011). Bismark: A flexible aligner and methylation caller for
656   Bisulfite-Seq applications. *Bioinformatics*, *27*(11), 1571–1572.
657   https://doi.org/10.1093/bioinformatics/btr167

658 Kuhn, M. (2019). *The caret Package*. https://topepo.github.io/caret/

659 Levine, M. E., Lu, A. T., Quach, A., Chen, B. H., Assimes, T. L., Bandinelli, S., Hou, L.,
660   Baccarelli, A. A., Stewart, J. D., Li, Y., Whitsel, E. A., Wilson, J. G., Reiner, A. P., Aviv,
661   A., Lohman, K., Liu, Y., Ferrucci, L., & Horvath, S. (2018). An epigenetic biomarker of
662   aging for lifespan and healthspan. *Aging (Albany NY)*, *10*(4), 573–591.
663   https://doi.org/10.18632/aging.101414

664 Levine, M., McDevitt, R. A., Meer, M., Perdue, K., Di Francesco, A., Meade, T., Farrell, C.,
665   Thrush, K., Wang, M., Dunn, C., Pellegrini, M., de Cabo, R., & Ferrucci, L. (2020). A rat
666   epigenetic clock recapitulates phenotypic aging and co-localizes with heterochromatin.
667   *ELife*, *9*, e59201. https://doi.org/10/ghjwd5

668 Levine, M., Serio, N., Radaram, B., Chaudhuri, S., & Talbert, W. (2015). Addressing the STEM
669   Gender Gap by Designing and Implementing an Educational Outreach Chemistry Camp
670   for Middle School Girls. *Journal of Chemical Education*, *92*(10), 1639–1644.
671   https://doi.org/10.1021/ed500945g

672 Lu, A. T., Quach, A., Wilson, J. G., Reiner, A. P., Aviv, A., Raj, K., Hou, L., Baccarelli, A. A.,
673   Li, Y., Stewart, J. D., Whitsel, E. A., Assimes, T. L., Ferrucci, L., & Horvath, S. (2019).
674   DNA methylation GrimAge strongly predicts lifespan and healthspan. *Aging*, *11*(2), 303–
675   327. https://doi.org/10.18632/aging.101684

676 Marini, S., Davis, K. A., Soare, T. W., Zhu, Y., Suderman, M. J., Simpkin, A. J., Smith, A. D. A.
677   C., Wolf, E. J., Relton, C. L., & Dunn, E. C. (2020). Adversity exposure during sensitive
678   periods predicts accelerated epigenetic aging in children. *Psychoneuroendocrinology*, *113*,
679   104484. https://doi.org/10.1016/j.psyneuen.2019.104484

680 Marioni, R. E., Harris, S. E., Shah, S., McRae, A. F., von Zglinicki, T., Martin-Ruiz, C., Wray, N.
681   R., Visscher, P. M., & Deary, I. J. (2016). The epigenetic clock and telomere length are
682   independently associated with chronological age and mortality. *International Journal of*
683   *Epidemiology*, *45*(2), 424–432. https://doi.org/10.1093/ije/dyw041

684 Marioni, R. E., Shah, S., McRae, A. F., Ritchie, S. J., Muniz-Terrera, G., Harris, S. E., Gibson, J.,
685   Redmond, P., Cox, S. R., Pattie, A., Corley, J., Taylor, A., Murphy, L., Starr, J. M.,
686   Horvath, S., Visscher, P. M., Wray, N. R., & Deary, I. J. (2015). The epigenetic clock is
687   correlated with physical and cognitive fitness in the Lothian Birth Cohort 1936.
688   *International Journal of Epidemiology*, *44*(4), 1388–1396.
689   https://doi.org/10.1093/ije/dyu277

690 Martin, M. (2011). Cutadapt removes adapter sequences from high-throughput sequencing reads.
691   *EMBnet.Journal*, *17*(1), 10. https://doi.org/10.14806/ej.17.1.200

692 Mattison, J. A., Colman, R. J., Beasley, T. M., Allison, D. B., Kemnitz, J. W., Roth, G. S.,
693   Ingram, D. K., Weindruch, R., de Cabo, R., & Anderson, R. M. (2017). Caloric restriction

694 improves health and survival of rhesus monkeys. *Nature Communications*, *8*, 14063.
695 https://doi.org/10.1038/ncomms14063

696 McCrory, C., Fiorito, G., O'Halloran, A. M., Polidoro, S., Vineis, P., & Kenny, R. A. (2022).
697 Early life adversity and age acceleration at mid-life and older ages indexed using the next-
698 generation GrimAge and Pace of Aging epigenetic clocks. *Psychoneuroendocrinology*,
699 *137*, 105643. https://doi.org/10.1016/j.psyneuen.2021.105643

700 Meer, M. V., Podolskiy, D. I., Tyshkovskiy, A., & Gladyshev, V. N. (2018). A whole lifespan
701 mouse multi-tissue DNA methylation clock. *ELife*, *7*, e40675.
702 https://doi.org/10.7554/eLife.40675

703 Meissner, A. (2005). Reduced representation bisulfite sequencing for comparative high-resolution
704 DNA methylation analysis. *Nucleic Acids Research*, *33*(18), 5868–5877.
705 https://doi.org/10.1093/nar/gki901

706 Mozhui, K., & Pandey, A. K. (2017). Conserved effect of aging on DNA methylation and
707 association with EZH2 polycomb protein in mice and humans. *Mechanisms of Ageing and
708 Development*, *162*, 27–37. https://doi.org/10.1016/j.mad.2017.02.006

709 National Center for Health Statistics, United States. (2021). *Life expectancy at birth and at age
710 65, by sex: Organisation for Economic Co-operation and Development (OECD)
711 countries, selected years 1980–2015.* (Table 14). CDC/NCHS.

712 Ong, M.-L., Tan, P. Y., MacIsaac, J. L., Mah, S. M., Buschdorf, J. P., Cheong, C. Y., Stunkel,
713 W., Chan, L., Gluckman, P. D., Chng, K., Kobor, M. S., Meaney, M. J., & Holbrook, J. D.
714 (2014). Infinium Monkeys: Infinium 450K Array for the Cynomolgus macaque (*Macaca
715 fascicularis*). *G3 Genes|Genomes|Genetics*, *4*(7), 1227–1234.
716 https://doi.org/10.1534/g3.114.010967

717 Pegoraro, M., Bafna, A., Davies, N. J., Shuker, D. M., & Tauber, E. (2016). DNA methylation
718 changes induced by long and short photoperiods in *Nasonia*. *Genome Research*, *26*(2),
719 203–210. https://doi.org/10.1101/gr.196204.115

720 Pichon, F., Shen, Y., Busato, F., P Jochems, S., Jacquelin, B., Grand, R. L., Deleuze, J.-F.,
721 Müller-Trutwin, M., & Tost, J. (2021). Analysis and annotation of DNA methylation in
722 two nonhuman primate species using the Infinium Human Methylation 450K and EPIC
723 BeadChips. *Epigenomics*, *13*(3), 169–186. https://doi.org/10.2217/epi-2020-0200

724 Pinho, G. M., Martin, J. G. A., Farrell, C., Haghani, A., Zoller, J. A., Zhang, J., Snir, S.,
725 Pellegrini, M., Wayne, R. K., Blumstein, D. T., & Horvath, S. (2022). Hibernation slows
726 epigenetic ageing in yellow-bellied marmots. *Nature Ecology & Evolution*, *6*(4), 418–426.
727 https://doi.org/10.1038/s41559-022-01679-1

728 Platt, A., Gugger, P. F., Pellegrini, M., & Sork, V. L. (2015). Genome-wide signature of local
729 adaptation linked to variable CpG methylation in oak populations. *Molecular Ecology*,
730 *24*(15), 3823–3830. https://doi.org/10.1111/mec.13230

731   Quinlan, A. R., & Hall, I. M. (2010). BEDTools: A flexible suite of utilities for comparing
732   genomic features. *Bioinformatics*, *26*(6), 841–842.
733   https://doi.org/10.1093/bioinformatics/btq033

734   Rawlins, R. G., & Kessler, M. J. (1986). *The Cayo Santiago macaques: History, behavior, and*
735   *biology*. State University of New York Press.

736   RStudio Team. (2015). *RStudio: Integrated Development for R*. RStudio, Inc.
737   http://www.rstudio.com/

738   Sapolsky, R. M. (2005). The Influence of Social Hierarchy on Primate Health. *Science*,
739   *308*(5722), 648–652. https://doi.org/10/fpfksr

740   Snyder-Mackler, N., Burger, J. R., Gaydosh, L., Belsky, D. W., Noppert, G. A., Campos, F. A.,
741   Bartolomucci, A., Yang, Y. C., Aiello, A. E., O'Rand, A., Harris, K. M., Shively, C. A.,
742   Alberts, S. C., & Tung, J. (2020). Social determinants of health and survival in humans
743   and other animals. *Science*, *368*(6493), eaax9553. https://doi.org/10.1126/science.aax9553

744   Snyder-Mackler, N., Sanz, J., Kohn, J. N., Brinkworth, J. F., Morrow, S., Shaver, A. O., Grenier,
745   J.-C., Pique-Regi, R., Johnson, Z. P., Wilson, M. E., Barreiro, L. B., & Tung, J. (2016).
746   Social status alters immune regulation and response to infection in macaques. *Science*,
747   *354*(6315), 1041–1045. https://doi.org/10.1126/science.aah3580

748   Spiers, H., Hannon, E., Wells, S., Williams, B., Fernandes, C., & Mill, J. (2016). Age-associated
749   changes in DNA methylation across multiple tissues in an inbred mouse model.
750   *Mechanisms of Ageing and Development*, *154*, 20–23.
751   https://doi.org/10.1016/j.mad.2016.02.001

752   Stubbs, T. M., Bonder, Marc Jan, Anne-Katrien Stark, Felix Krueger, BI Ageing Clock Team,
753   von Meyenn, F., Stegle, O., & Reik, W. (2017). Multi-tissue DNA methylation age
754   predictor in mouse. *Genome Biology*, *18*(1). https://doi.org/10.1186/s13059-017-1203-5

755   Susman, E. J., Houts, R. M., Steinberg, L., Belsky, J., Cauffman, E., DeHart, G., Friedman, S. L.,
756   Roisman, G. I., Halpern-Felsher, B. L., & for the Eunice Kennedy Shriver NICHD Early
757   Child Care Research Network. (2010). Longitudinal Development of Secondary Sexual
758   Characteristics in Girls and Boys Between Ages 9½ and 15½ Years. *Archives of*
759   *Pediatrics & Adolescent Medicine*, *164*(2), 166.
760   https://doi.org/10.1001/archpediatrics.2009.261

761   Tange, O. (2018). *Gnu Parallel 2018*. Zenodo. https://doi.org/10.5281/ZENODO.1146014

762   Tarandovskiy, I. D., Shin, H. K. H., Baek, J. H., Karnaukhova, E., & Buehler, P. W. (2020).
763   Interspecies comparison of simultaneous thrombin and plasmin generation. *Scientific*
764   *Reports*, *10*(1), 3885. https://doi.org/10.1038/s41598-020-60436-1

765   Teschendorff, A. E., & Relton, C. L. (2018). Statistical and integrative system-level analysis of
766   DNA methylation data. *Nature Reviews Genetics*, *19*(3), 129–147.
767   https://doi.org/10.1038/nrg.2017.86

768   Wang, T., Tsui, B., Kreisberg, J. F., Robertson, N. A., Gross, A. M., Yu, M. K., Carter, H.,
769   Brown-Borg, H. M., Adams, P. D., & Ideker, T. (2017). Epigenetic aging signatures in

29

770   mice livers are slowed by dwarfism, calorie restriction and rapamycin treatment. *Genome*
771   *Biology*, *18*(1). https://doi.org/10.1186/s13059-017-1186-2

772 Watowich, M. M., Chiou, K. L., Montague, M. J., Cayo Biobank Research Unit, Simons, N. D.,
773   Horvath, J. E., Ruiz-Lambides, A. V., Martínez, M. I., Higham, J. P., Brent, L. J. N., Platt,
774   M. L., Snyder-Mackler, N., Brent, L. J. N., Higham, J. P., Martínez, M. I., Montague, M.
775   J., Platt, M. L., & Snyder-Mackler, N. (2022). Natural disaster and immunological aging
776   in a nonhuman primate. *Proceedings of the National Academy of Sciences*, *119*(8),
777   e2121663119. https://doi.org/10.1073/pnas.2121663119

778 Wilkinson, G. S., Adams, D. M., Haghani, A., Lu, A. T., Zoller, J., Breeze, C. E., Arnold, B. D.,
779   Ball, H. C., Carter, G. G., Cooper, L. N., Dechmann, D. K. N., Devanna, P., Fasel, N. J.,
780   Galazyuk, A. V., Günther, L., Hurme, E., Jones, G., Knörnschild, M., Lattenkamp, E. Z.,
781   … Horvath, S. (2021). DNA methylation predicts age and provides insight into
782   exceptional longevity of bats. *Nature Communications*, *12*(1), 1615.
783   https://doi.org/10.1038/s41467-021-21900-2

784 Wu, G., Feng, X., & Stein, L. (2010). A human functional protein interaction network and its
785   application to cancer data analysis. *Genome Biology*, *11*(5), R53.
786   https://doi.org/10.1186/gb-2010-11-5-r53

787 Yang, Z., Wong, A., Kuh, D., Paul, D. S., Rakyan, V. K., Leslie, R. D., Zheng, S. C.,
788   Widschwendter, M., Beck, S., & Teschendorff, A. E. (2016). Correlation of an epigenetic
789   mitotic clock with cancer risk. *Genome Biology*, *17*(1), 205.
790   https://doi.org/10.1186/s13059-016-1064-3

791 Zhang, W., Spector, T. D., Deloukas, P., Bell, J. T., & Engelhardt, B. E. (2015). Predicting
792   genome-wide DNA methylation using methylation marks, genomic position, and DNA
793   regulatory elements. *Genome Biology*, *16*(1), 14. https://doi.org/10.1186/s13059-015-
794   0581-9

795 Zhang, Y., Baheti, S., & Sun, Z. (2016). Statistical method evaluation for differentially
796   methylated CpGs in base resolution next-generation DNA sequencing data. *Briefings in*
797   *Bioinformatics*, bbw133. https://doi.org/10.1093/bib/bbw133

798 Zheng, Y., Joyce, B. T., Colicino, E., Liu, L., Zhang, W., Dai, Q., Shrubsole, M. J., Kibbe, W. A.,
799   Gao, T., Zhang, Z., Jafari, N., Vokonas, P., Schwartz, J., Baccarelli, A. A., & Hou, L.
800   (2016). Blood Epigenetic Age may Predict Cancer Incidence and Mortality.
801   *EBioMedicine*, *5*, 68–73. https://doi.org/10.1016/j.ebiom.2016.02.008

802 Zou, H., & Hastie, T. (2005). Regularization and variable selection via the elastic net. *Journal of*
803   *the Royal Statistical Society: Series B (Statistical Methodology)*, *67*(2), 301–320.
804   https://doi.org/10.1111/j.1467-9868.2005.00503.x

805 Zou, L. S., Erdos, M. R., Taylor, D. L., Chines, P. S., Varshney, A., Parker, S. C. J., Collins, F.
806   S., The McDonnell Genome Institute, & Didion, J. P. (2018). BoostMe accurately predicts
807   DNA methylation values in whole-genome bisulfite sequencing of multiple human
808   tissues. *BMC Genomics*, *19*(1), 390. https://doi.org/10.1186/s12864-018-4766-y

809

810
811
DATA ACCESSIBILITY STATEMENT
813
Code for all analyses can be found on GitHub (https://github.com/elisabethgoldman/RheMacAge) and data are accessible on NCBI SRA through BioProject accession PRJNA610241.
816
817
AUTHOR CONTRIBUTIONS
819
NSM, KNS, LJNB, JPH, and EAG conceptualized the research; Sample collection on Cayo Santiago was facilitated by KLC, JEH, MIM, MJM, JPH, LJNB, MLP, and NSM; KLC, AM, and SNS performed genomic lab work; behavioral data collection on Cayo Santiago was coordinated and led by LJNB; sample collection from the Yerkes Primate Research Center was facilitated by NSM and JT; JT oversaw data collection from the baboons at Amboseli; EAG, KLC, and MMW performed genomic analysis with input from NSM, JT, and JAA; EAG, KLC, MMW, KNS, and NSM wrote the manuscript. All authors reviewed and revised the manuscript.
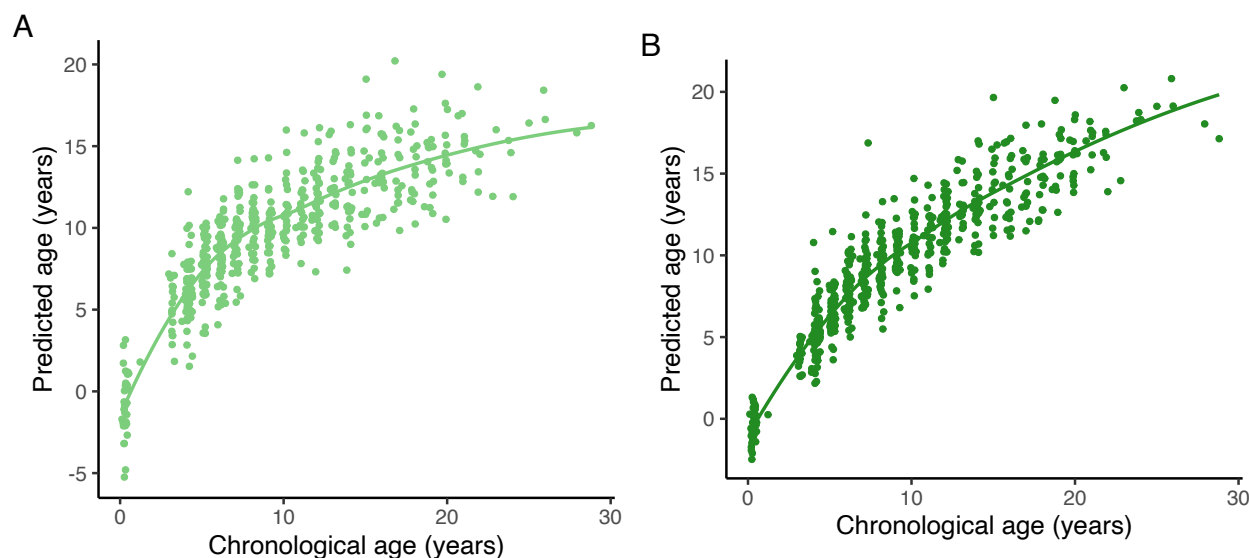827
828
829
830
831
832
833
834
835
836
837
838
839
840
841
842

843   **FIGURES**

844
845
846   **Figure 1 Comparison of Site-Based and Sliding Window-Based Models**
847
848   **(A) Site-based model of methylation age successfully predicts known chronological age.**
849   Known chronological age is highly correlated with epigenetic age predictions from our site-based
850   epigenetic clock (Pearson's r = 0.82, median absolute deviation between predicted and
851   chronological age [MAD] = 2.11 years). Methylation data used to generate the site- and window-
852   based clocks are from whole blood samples from a cross-sectional sample of rhesus macaques
853   living on the island of Cayo Santiago (n samples = 549; n unique females = 267, n unique males
854   = 217). Curved line shows line of best fit from univariate loess regression.
855
856   **(B) Window-based model of methylation age successfully predicts known chronological age**
857   **and outperforms the site-based model.** Known chronological age is more highly correlated
858   with epigenetic age predictions in the window-based epigenetic clock (Pearson's r = 0.9, MAD =
859   1.42 years) than the site-based clock. The model was generated using whole blood samples from
860   rhesus macaque living on the island of Cayo Santiago (n samples = 563; n unique females = 273,
861   n unique males = 220). Curved line shows line of best fit from univariate loess regression.
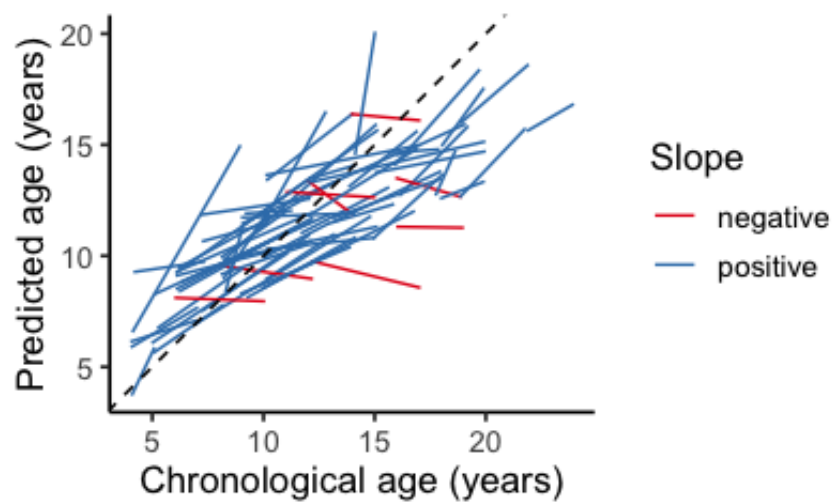862

863

Figure 2 Predicted Aging Trajectories for Repeatedly Sampled Individuals

Predicted age increased over time in repeatedly sampled individuals (n = 66 individuals). 88.6% of epigenetic age predictions were higher in the sample collected when the individual was older (blue lines; 62/70 predictions; p = 9.13 x 10^{-12}, one-sided exact binomial test). Dashed line shows x=y.
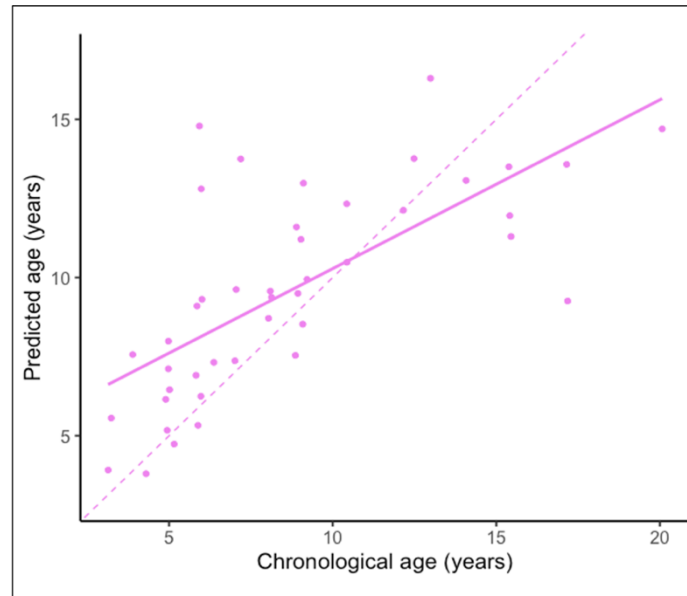
873
874
875 **Figure 3 Predicted DNA Methylation Age for Yerkes Macaques Using RheMacAge Model**
876
877 Predicted DNA methylation age for Yerkes rhesus macaques is correlated with chronological age
878 (r = 0.69, MAD = 2.09 years). Solid line shows line of best fit from a univariate linear regression
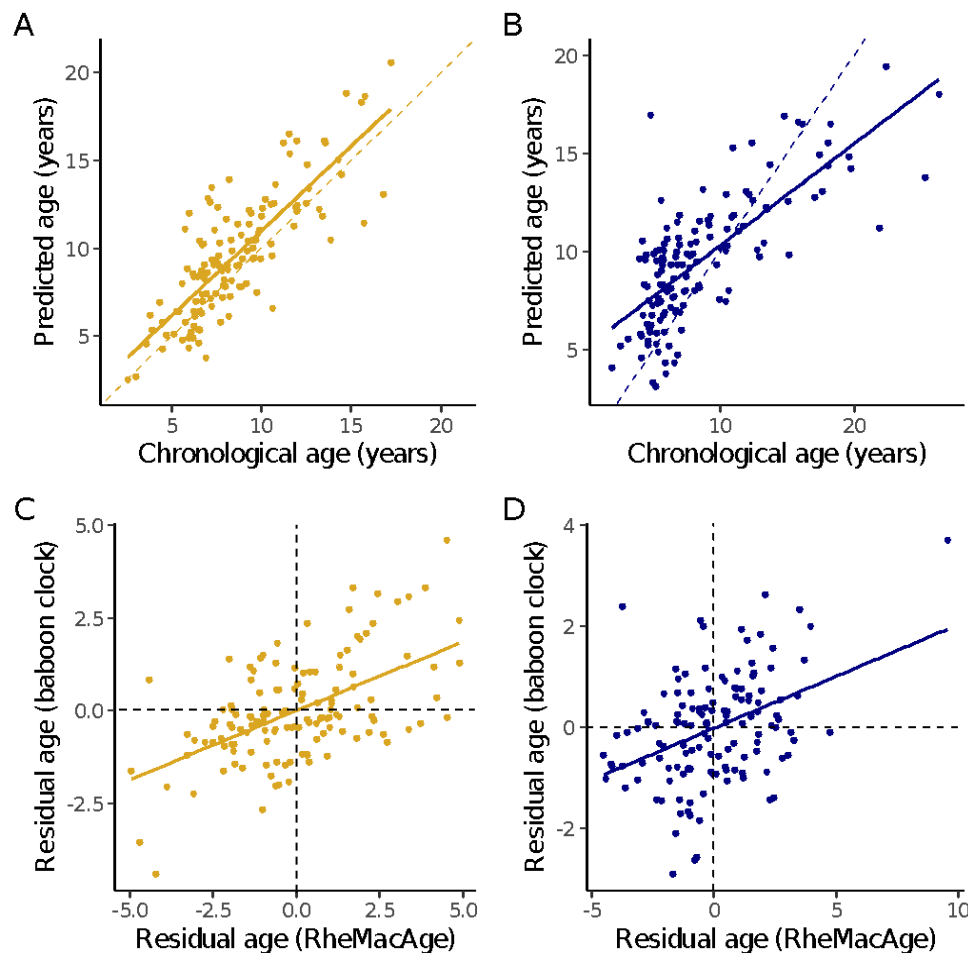879 of predicted age onto chronological age.
880

Figure 4 Predicted DNA Methylation Age for Amboseli Baboons Using RheMacAge Model

RheMacAge successfully predicts interspecies epigenetic ages from baboon DNA methylation data and recapitulates results from a baboon-specific methylation clock. Predicted age for **(A)** male and **(B)** female baboons using the RheMacAge epigenetic clock are highly correlated with known chronological age (males: r = 0.8, MAD = 1.34 years; females: r = 0.74, MAD = 2.19 years). The solid line shows the line of best fit from univariate linear regression of predicted onto chronological age. Dashed line shows x = y. Residual epigenetic age from the RheMacAge (x-axis) recapitulates residual ages from a baboon-specific clock (y-axis) for **(C)** males (r = 0.55, p = 5.28 x 10^{-12}) and **(D)** females (r = 0.41, p = 7.49 x 10^{-7}). Points in the bottom left (decelerated ages) and top right (accelerated ages) quadrants reflect concordance in residual epigenetic ages between the two clocks. Discordant predictions between the two clocks (i.e., one clock predicts accelerated age while the other predicts decelerated rate of aging) are in the top left and bottom right quadrants.